AD 297 526

19990929035

ASRL TR 94-3

PLASTIC DEFORMATION OF THIN BRAZED JOINTS IN SHEAR

by

C. W. SHAW, L. A. SHEPARD

and

J. A. WULFF

MASSACHUSETTS INSTITUTE OF TECHNOLOGY

AEROELASTIC AND STRUCTURES RESEARCH LABORATORY

DEPARTMENT OF AERONAUTICS AND ASTRONAUTICS

AND

METALS PROCESSING DIVISION

METALLURGY DEPARTMENT

NOVEMBER 1962

OFFICE OF SCIENTIFIC RESEARCH

AIR RESEARCH AND DEVELOPMENT COMMAND

UNITED STATES AIR FORCE

PLASTIC DEFORMATION OF THIN BRAZED JOINTS IN SHEAR

by

C. W. Shaw, L. A. Shepard and J. Wulff

MASSACHUSETTS INSTITUTE OF TECHNOLOGY
AEROELASTIC AND STRUCTURES RESEARCH LABORATORY
DEPARTMENT OF AERONAUTICS AND ASTRONAUTICS
AND
METALS PROCESSING DIVISION
METALLURGY DEPARTMENT

•

Contract No. AF 49(638)-775
Project No. 9782
Task No. 37718

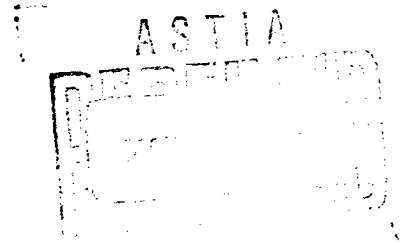

November 1962

OFFICE OF SCIENTIFIC RESEARCH
AIR RESEARCH AND DEVELOPMENT COMMAND
UNITED STATES AIR FORCE

Bibliographical Control Sheet

1. Originating Agency and Monitoring Agency:
   O.A.: Massachusetts Institute of Technology
   Cambridge, Massachusetts
   M.A.: Office of Scientific Research, Air Research and Development Command, USAF

2. Originating Agency Report Number:
   MIT, Aeroelastic and Structures Research Laboratory
   TR 94-3

3. Title and Classification of Title:
   PLASTIC DEFORMATION OF THIN BRAZED JOINTS IN SHEAR (UNCLASSIFIED)

4. Personal Authors: C. W. Shaw, L. A. Shepard, J. Wulff

5. Date of Report: November 1962

6. Pages: 52

7. Illustrative Material: 20

8. Prepared for Contract No.: AF 49(638)-775

9. Prepared for Project Code and/or No. 9782

10. Security Classification: UNCLASSIFIED

11. Distribution Limitations: None

12. Abstract:

The plastic behavior of the more ductile phase of a two phase material was simulated in shear tests on thin silver joints brazed in tubular steel specimens. Both the yield

strength and the work hardening rate of the silver were increased by the presence of the rigid interfaces. At 10 percent strain, the flow stress of the thin joints was 1 1/2 as great as fine grained polycrystalline silver.

Deformations of the silver near the steel interfaces was severely limited even at large strains, resulting in a gross strain inhomogeneity across the joint. These effects were postulated to arise from the constraint of slip by the non-yielding interfaces.

FOREWORD

The authors wish to acknowledge the interest and support of the personnel of the Office of Scientific Research in this study of composite material properties. Their appreciation is tendered to Professors E. Orowan and J. Mar for their helpful suggestions and criticisms. Mr. Ray Waldman is thanked for aiding in photomicrography.

ABSTRACT

The plastic behavior of the more ductile phase of a two phase material was simulated in shear tests on thin silver joints brazed in tubular steel specimens. Both the yield strength and the work hardening rate of the silver were increased by the presence of the rigid interfaces. At 10 percent strain, the flow stress of the thin joints was 1 1/2 as great as fine grained polycrystalline silver.

Deformations of the silver near the steel interfaces was severely limited even at large strains, resulting in a gross strain inhomogeneity across the joint. These effects were postulated to arise from the constraint of slip by the non-yielding interfaces.

TABLE OF CONTENTS

LIST OF FIGURES

LIST OF FIGURES (continued)

INTRODUCTION

General understanding of the plastic deformation processes in two phase materials is still rudimentary. This is especially true in reference to materials in which the stronger phase makes up a reasonably large fraction of the volume. It is well known, from current studies,[1,2] that the flow stress of the weaker phase is considerably enhanced over its normal unconstrained strength. However, this strengthening is thought to arise mainly from a hydrostatic component which cannot contribute to the plastic straining. An estimate of the plastic deformation characteristics of the softer phase in a two phase material must, for want of both data and theory in this field, be largely inferred from an analogy with polycrystalline single phase metals.

The plastic behavior of a grain in a polycrystal is governed primarily by the macroscopic requirement of strain continuity with the grains which surround it.[3] In face centered cubic metals, this factor has been shown to be the major cause of the higher work hardening rate of polycrystals in comparison with single crystals. Orientation of an individual grain relative to the stress axis, while dictating the initial slip systems which will be active, does not prescribe the amount of slip which will occur on each. There is no statistical correlation between the gross strain increment of each grain and its orientation at any stage of deformation.[4,5] Furthermore, different regions of one grain have been shown to deform and work harden by different amounts[6,7] and on different sets of slip systems.[8] This inhomogeneous deformation occurs to preserve strain continuity and, therefore, boundary contiguity with neighboring grains.

A secondary but significant factor influencing the work hardening of polycrystalline metals is the relaxation of local stress concentrations across a grain boundary. Although slip

dislocations cannot pass through a grain boundary, they can move to within a few atom distances of the boundary under stresses of the order of the yield stress.[9] Subsequent dislocations from the same source will pile up on the slip plane. The elastic repulsion between piled up dislocations will produce two effects. It will relax the applied shear stress τ_a on the source so that a maximum number of edge dislocations, n, that can be piled up over the distance L between the source and the boundary is[10]

$$n = \frac{\pi L \tau_a (1-\nu)}{\mu b} \quad . \qquad (1)$$

where ν = Poisson's ratio
μ = shear modulus
b = Burger's vector

And, it will exert a local stress concentration on the neighboring grain at the boundary. The second grain is observed to slip on planes most favorably oriented to relax this stress concentration.[11] As a result of this process, a layer of multiple slip is developed near the grain boundaries which is apparently responsible for the increased strength of polycrystals with decreasing grain size.[12,13]

A comparison of these observations for pure polycrystalline metals with the few available results for two phase metals indicates a reasonably close parallel. Honeycombe and Boas[14] and Clarebrough[15] studied the distribution of deformation in two phase alloys by observing recrystallization behavior. It was found that recrystallization in the softer phase initiated in regions away from the hard phase interface indicating that the degree of deformation increased away from the interface. This observation is in accord with the strain continuity requirements noted previously for single phase polycrystals. However, the experimental procedure is too indirect to allow a positive conclusion.

Head[16] has analyzed the distribution of piled up dislocations in a material of shear modulus μ_1 against a boundary with a material of higher modulus μ_2. The abrupt change in elastic stress field results in the repulsion of dislocations from the boundary. Therefore, the distance between the lead dislocation and the boundary is increased by an order of magnitude or more (depending upon the values of the moduli) over that for an ordinary grain boundary under comparable stresses. However, the applied stress, τ_a, required to pile up n dislocations in a distance L is not increased appreciably over the value given by Eq. 1 for a grain boundary. For example, with $\mu_2/\mu_1 = 3$, τ_a is increased by a factor of ~ 1.5 for four dislocations, ~ 1.3 for sixteen and progressively smaller amounts for larger numbers of piled up dislocations over the values determined for Eq. 1. A more important distinction for the two phase boundary case is that stresses due to the pileups are not relaxed unless the more rigid material deforms plastically.

The need for further experimental investigation into the plastic deformation characteristics of two phase materials is evident. In the present study, this problem was approached in an elementary form. Hollow tubular specimens consisting of thin silver wafers brazed between steel grips were tested in torsion. The shear characteristics of silver joints ranging in thickness from 0.001 to 0.1 inches were compared with those of fine grained polycrystalline silver.

SPECIMEN PREPARATION

The torsion specimen with a silver ring brazed at its midlength is shown in Fig. 1b. Specimen preparation followed generally the procedure outlined by Moffatt and Wulff.[17] Two and one-half inch square blocks of 1075 steel were wet ground, lapped and polished on the surfaces to be joined. A count of interference fringes against an optical flat was made to check overall flatness of each block. In the areas from which the specimens were cut, deviations were held to less than 0.0001 inch.

The blocks were spaced at the edge for the desired joint thickness, and an excess of fine silver bar, 99.9^{+} percent purity, was placed in a hole through the center of the top block. The assembly was then brazed at 1050^{o}C through a carefully controlled heating cycle in a hydrogen muffle furnace.

Each set of brazed blocks was quartered and machined into four specimens as shown in Fig. 2. As the block cooled from the outside, long columnar grains were formed tapering from the surface to the central riser. The average joint contained three to five original grains, but four to eight grain boundaries, for sections of the same grain often appeared on diametrically opposite sides of the joint in the growth direction (Fig. 2). Grain boundaries extended completely across the joint, normal to the steel interfaces in all cases.

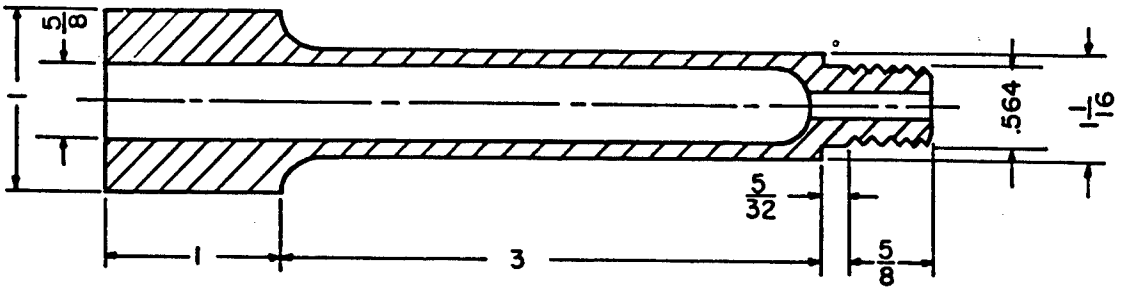

FIG IA

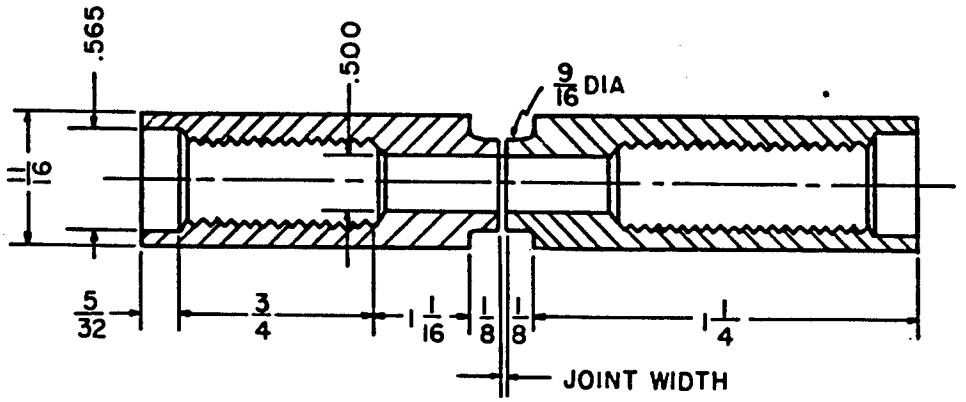

FIG IB

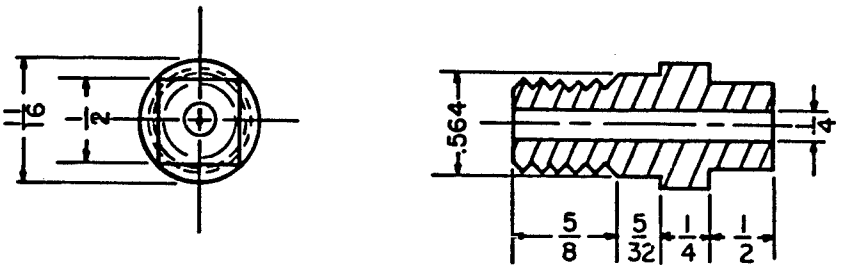

FIG IC

FIGURE 1 TORSION SPECIMEN AND THREADED END EXTENSIONS

A) HEAD STOCK EXTENSION AND TORQUE MEASURING TUBE

B) TORSION SPECIMEN

C) TAIL STOCK EXTENSION

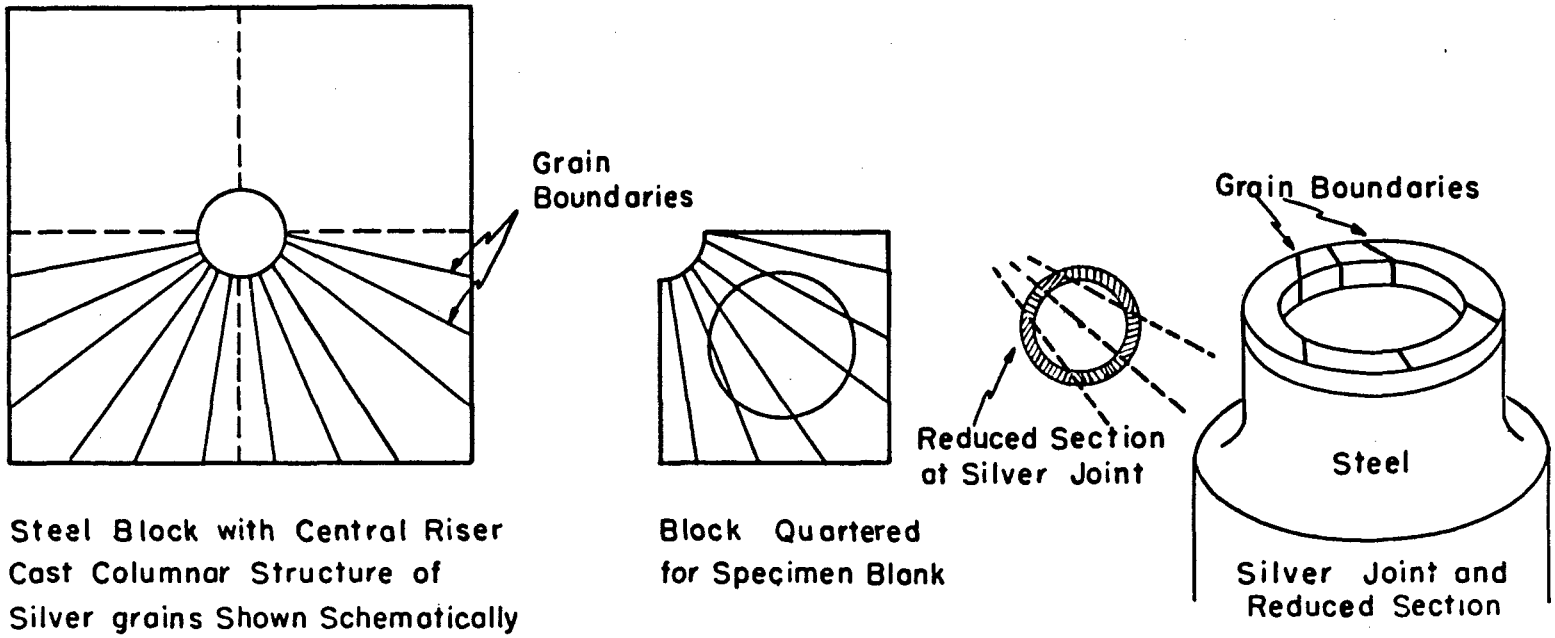

Fig. 2 Preparation of a Silver Brazed Joint Torsion Specimen
(Development of Silver Grain Structure Shown Schematically)

TESTING PROCEDURE

The torsion testing machine and associated stress and strain measuring devices were especially designed or adapted to cope with the unique problems associated with the testing of thin ductile joints. The final design of the apparatus, adopted after considerable experience with the problem, is discussed in detail in the Appendix.

The manually operated torsion unit is a gear-driven lathe modified with additional gears at the headstock to allow a twist of one degree on the specimen for a complete revolution of the hand wheel. A special coupling on the tail-stock end allowed transmission of torque to the specimen with the virtual elimination of all bending stresses and hydrostatic stresses.

Stress on the specimen was determined to an accuracy of ± 10 psi from the output of two 90° rosette strain gages mounted on the torque tube (Fig. 1A). A circular variable inductance a.c. potentiometer was used in the extensometer for displacement sensing. The position of the potentiometer was held fixed at one edge of the joint while the movement of the other edge was mechanically applied to displacement of the rotor. The weight of the extensometer was supported by bearings mounted on the specimen shoulders, while the relative motion of the two interfaces was transmitted by fine hardened points indented into the steel about 0.01 inches from the edge of the silver joint. With a linear output of two volts per degree of twist, angular displacements could be read to a sensitivity of 1/20,000 of a degree. For the chosen specimen dimensions the least reading of the extensometer represented a shear strain of 2×10^{-4} across a 0.001 inch thick joint, and 2×10^{-6} across a 0.100 inch joint.

The accuracy and sensitivity of the stress and strain measuring systems were checked by repeated measurements of the shear modulus on elastically strained steel tubes. Up to the

yield point, the readings deviated by less than $\pm$ 1 unit in the least reading from the average curve, and overall linearity was within 2 percent. Variations in the measured modulus of $\pm$ 2 percent from different samples were found to arise mainly from errors in measurement of specimen dimensions. The shear moduli of steel and silver measured with this apparatus are 11.4 and 3.76×10^6 psi respectively.

Prior to testing, the inner and outer diameters of the silver joint were measured. Joint thickness was determined at three points around the specimen using a filar eyepiece microscope. End grips, shown in Fig. 1, were screwed into the specimen and separately tightened, to a stress in excess of that applied during the test. The left-hand grip, Fig. 1A, served also as the torque tube. The assembly was carefully aligned in the torsion testing machine and the extensometer mounted upon the reduced section of the specimen.

Shear stress-shear strain curves for a series of samples varying in joint thickness from 0.001 to 0.100 inches and for two long polycrystalline silver tubes, 0.002 inch grain size, were measured using the precise extensometry described. (The polycrystalline tubes averaged 15 grains across the wall thickness in the radial direction.) Maximum strain in these tests was usually limited to less than 20 percent, as principal interest was focused upon the yield stress and early work hardening of the joint. However, a reasonable number of samples were tested to failure.

Throughout this report, the shear strain γ and the shear stress τ of the joint are defined as follows:

$$\gamma = \frac{\theta r_m}{t} \qquad \tau = \frac{T}{A r_m}$$

where θ = twist angle in radians
r_m = average of internal and external joint radii
t = joint thickness

T = applied torque

A = cross-sectional area of the joint

Deformation characteristics of individual grains of the joint were followed during the course of straining for a number of samples. The displacement of fine lines scribed across the joint was photographed after successive incremental strains.

RESULTS AND DISCUSSION

A. Deformation Characteristics of the Silver Joints

Data for the shear stress-shear strain (τ-γ) curves for the two polycrystalline silver tubes, and the silver joints are given in Table I. The curves are characterized by a region of rapid hardening from $\gamma = 0.0001$ to 0.01 followed by a lower, approximately linear hardening rate from $\gamma = 0.02$ to 0.10. The rate of work hardening at $\gamma = 0.05$ is shown in the right hand column.

The deformation characteristics of the two polycrystalline tubes differed somewhat, Sample A24 showing a higher initial rate of hardening and a smaller subsequent hardening than Sample A17. At larger strains, the two curves became approximately identical.

τ-γ curves for the silver joints fell into two groups, distinguished primarily by yield stress. Examples of curves for samples exhibiting the lower and higher yield behavior are compared with the curve for polycrystalline sample A24 in Figs. 3 and 4 respectively. Deformation of the thickest joints, t = 0.1 inches, was closely parallel to that of the polycrystalline samples of grain size 0.002 inches (e.g. A-22, Fig. 3). All thinner joints, excepting A-21, showed a higher rate of work hardening than the fine grained tubes, and exceeded the strength of the polycrystalline samples beyond 10 percent strain. Thus, the strength of the silver in the brazed joint was greater than that of polycrystalline silver, even in cases where the minimum dimension of the joint grain was a factor of ten or more greater than the polycrystal grain size. For joint thickness of the same order as the polycrystal grain size, the relative strength of the joint was magnified by a factor of 1.5 at 10 percent strain.

TABLE I

Yield and Flow Stress Data for the Shear of Brazed Silver Joints and Polycrystalline Silver Tubes

Specimen No. Ductile Joints	Joint Thickness Inches	Yield Stress psi = 0.0001	Flow Stress, psi				$\frac{d\tau}{d\gamma}$ γ=0.05
			γ = 0.001	γ = 0.005	γ = 0.01	γ = 0.10	
A-2	0.0009	3400	3850	6160	8130	16,800	82,500
A-3	0.0009	6700	7620	9300	10900	15,000	38,400
A-25	0.0011	5075	6120	7930	8880	13,350	43,900
A-4	0.0013	6070	6410	7380	8030	12,700	34,300
A-10	0.0017	8020	8400	9130	9760	13,200	34,200
A-23	0.0041	3550	4370	5600	6250	9,320	28,200
A-7	0.0043	5100	6560	7520	7980	10,680	27,200
A-27	0.0076	5800	7250	8710	9550	14,420	48,100
A-5	0.0086	5625	6680	8080	8770	12,600	36,200
A-8	0.0091	3375	4630	5700	6300	9,190	30,100
A-13	0.0108	3800	4570	5620	6060	9,190	30,800
A-21	0.0110	4835	5630	6460	6780	8,610	18,700
A-12	0.0235	3750	4800	5770	6220	9,410	34,100
A-20	0.0286	3875	6640	8130	8570	12,320	38,700
A-28	0.0282	3625	6640	-	-	-	
A-15	0.0979	1700	2840	-	-	-	
A-6	0.0979	3450	4830	5580	5860	7,400	15,900
A-22	0.0970	3150	5370	6860	7330	8,610	16,300
Polycrystalline Tubes	Grain Size						
A-24	0.0016	4400	6230	7140	7550	8,977	12,500
A-17	0.0020	4475	5420	5570	5650	7,560	20,200

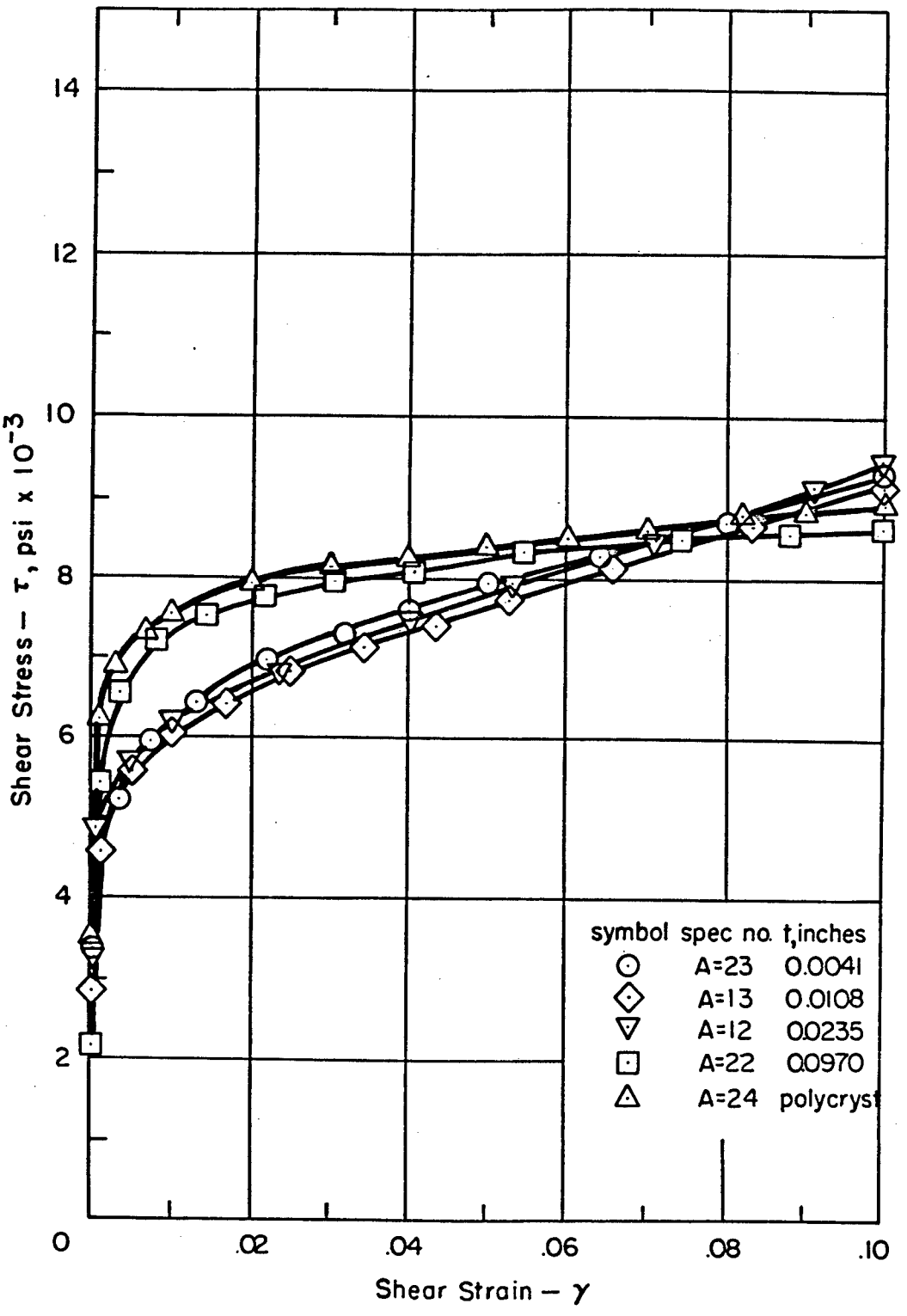

Fig. 3 Stress – Strain Curves for a Series of Silver Joint Specimens Compared with Polycrystalline Silver

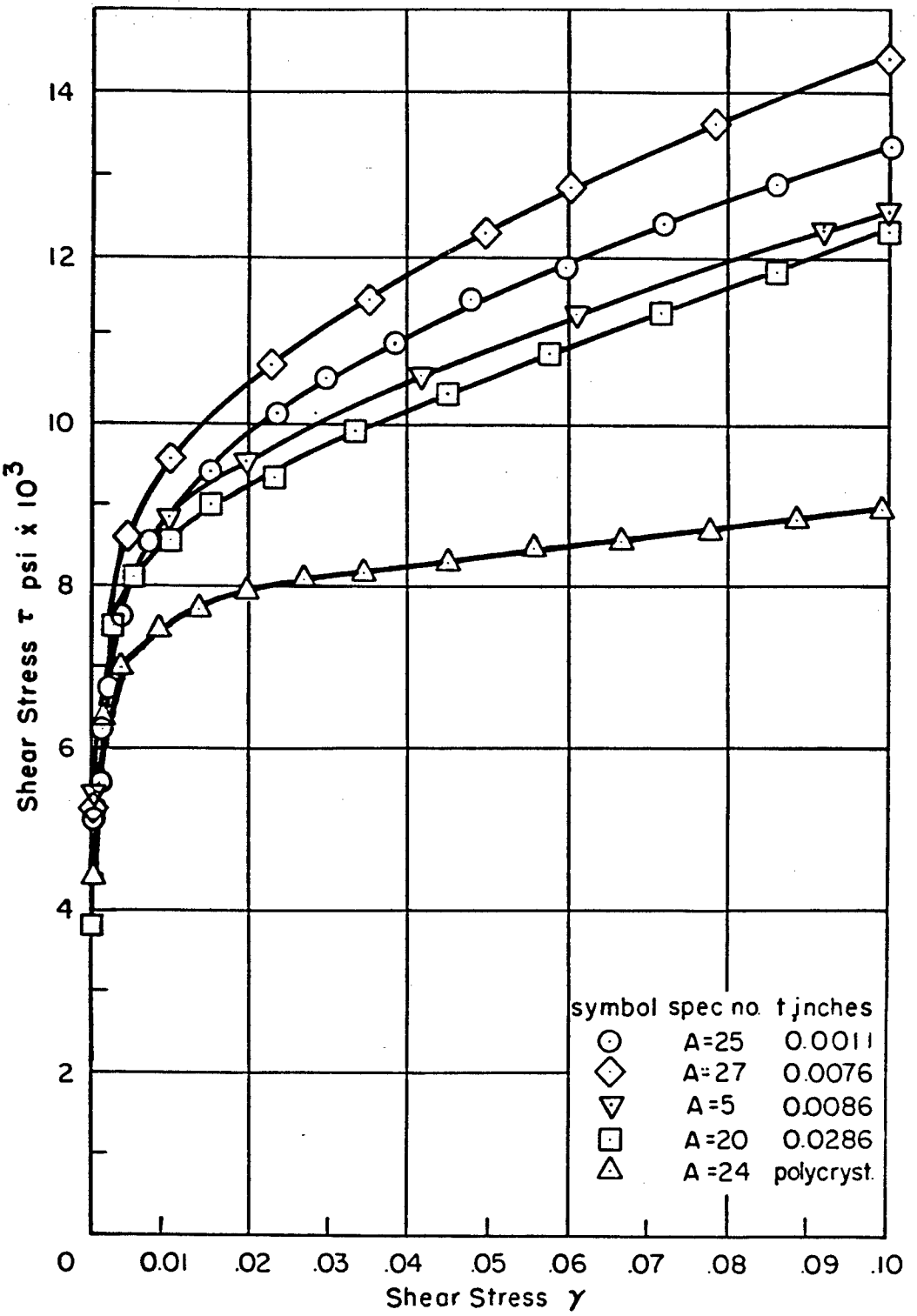

Fig. 4 Stress—Strain Curves for a Series of Silver Joint Specimens Compared with Polycrystalline Silver

It is apparent from Table I that the strength of a joint was not a unique function of its thickness. Observations of the deformation of individual grains of a joint revealed that the orientation of the grain relative to the steel interface is an important factor governing its strength, as will be discussed subsequently. Apparently the effect of the small sampling of grain orientations in the three to five grain silver joints outweighed the possible influence of joint thickness on strength in these tests. However, it will be noted that the 0.001 inch joints form a uniformly strong group, as demonstrated in Fig. 5.

At higher strains, the silver joints continued to work harden at an appreciable rate, Fig. 6. Stresses at fracture, Fig. 7,* showed a general trend, decreasing with increasing joint thickness. An average fracture strain $\gamma = 2.5$ was observed. Specimens fractured in the silver along the midplane of the joint. The 0.001 inch joints failed abruptly over the entire joint area.

B. Yield Behavior of the Silver Joints

The yield strengths ($\gamma = 0.0001$) of the silver joints fell into two groupings as already noted, Fig. 8: one of constant value independent of joint thickness, and the second rising roughly linearly with decreasing log joint thickness. As such large relative deviations are not ordinarily observed in the yielding of pure metals, the possibility that these differences arose from the interaction of slip with the steel interfaces at small strains was suggested. The sensitive extensometry allowed the resolution of plastic strains of the order of 10^{-6} for joints 0.025 inches thick and over. Determination of small strain behavior revealed that the joints show the initial high hardening rate associated with parabolic hardening over the strain range from

*Data for this figure was determined from an earlier set of tests in which less sensitive extensometry was used.

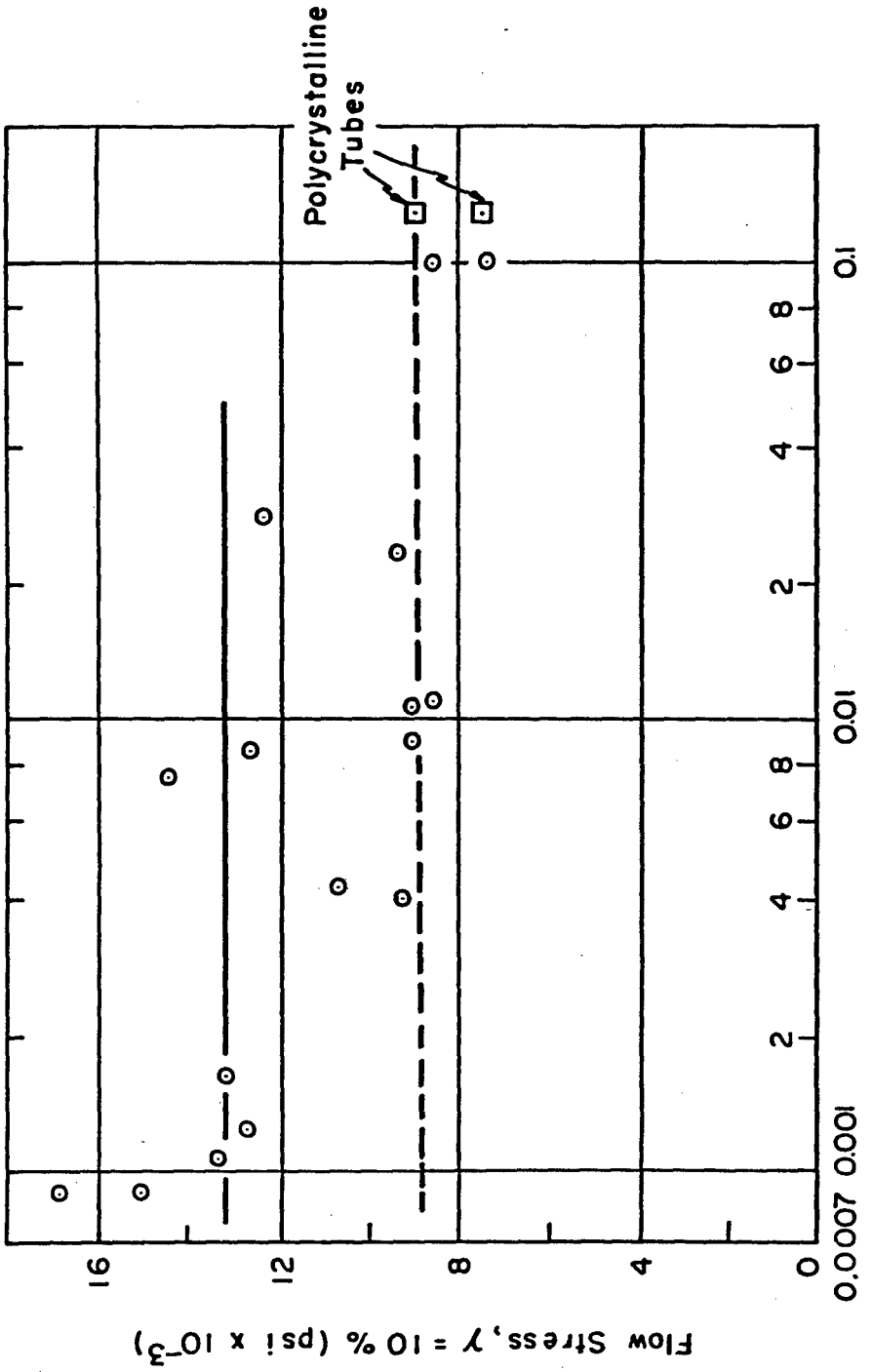

Fig. 5 Variation of Flow Stress, γ = 10 %, with Silver Joint Thickness

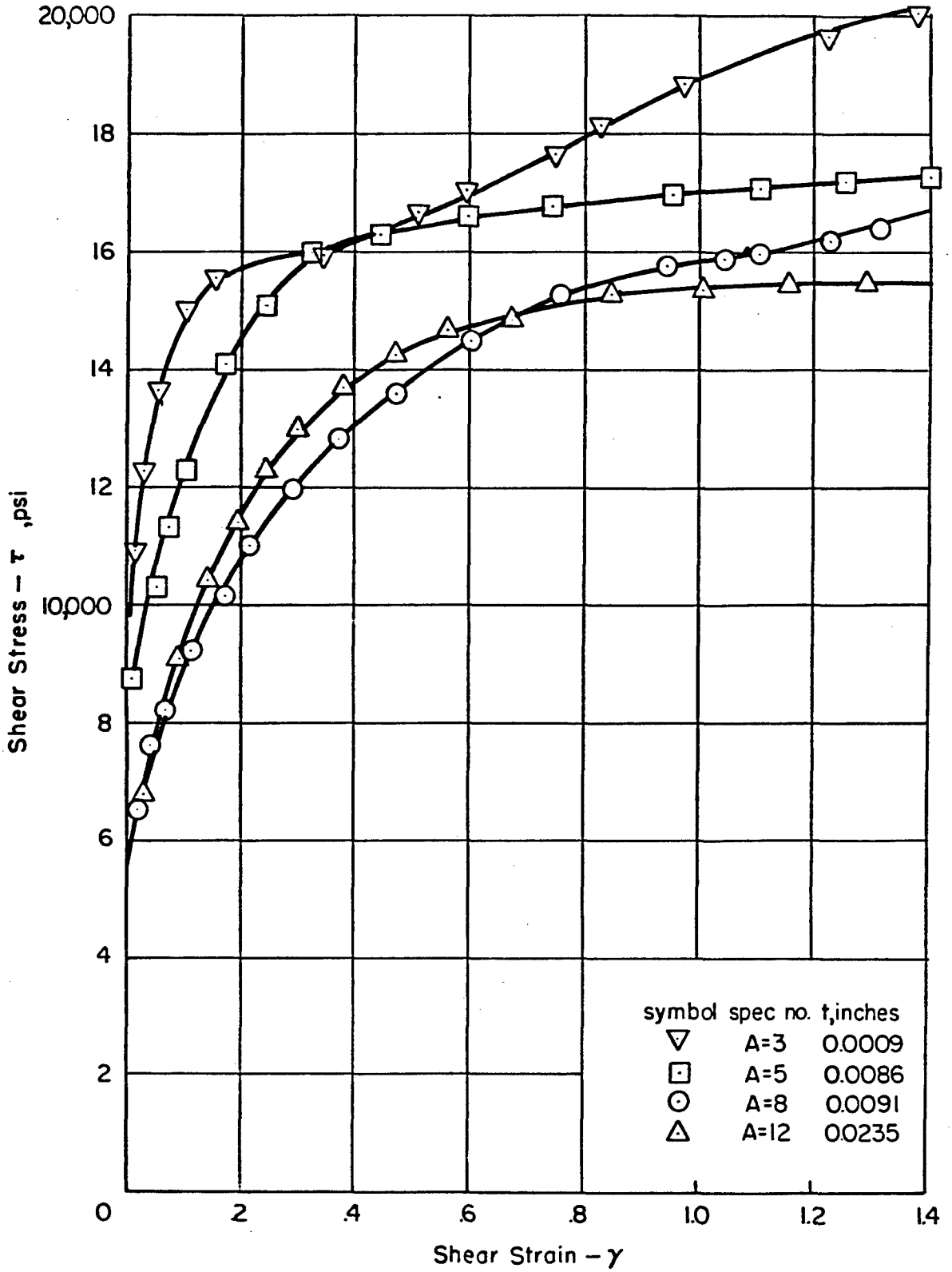

Fig. 6 Stress – Strain Curves for Silver Joints at Large Strains

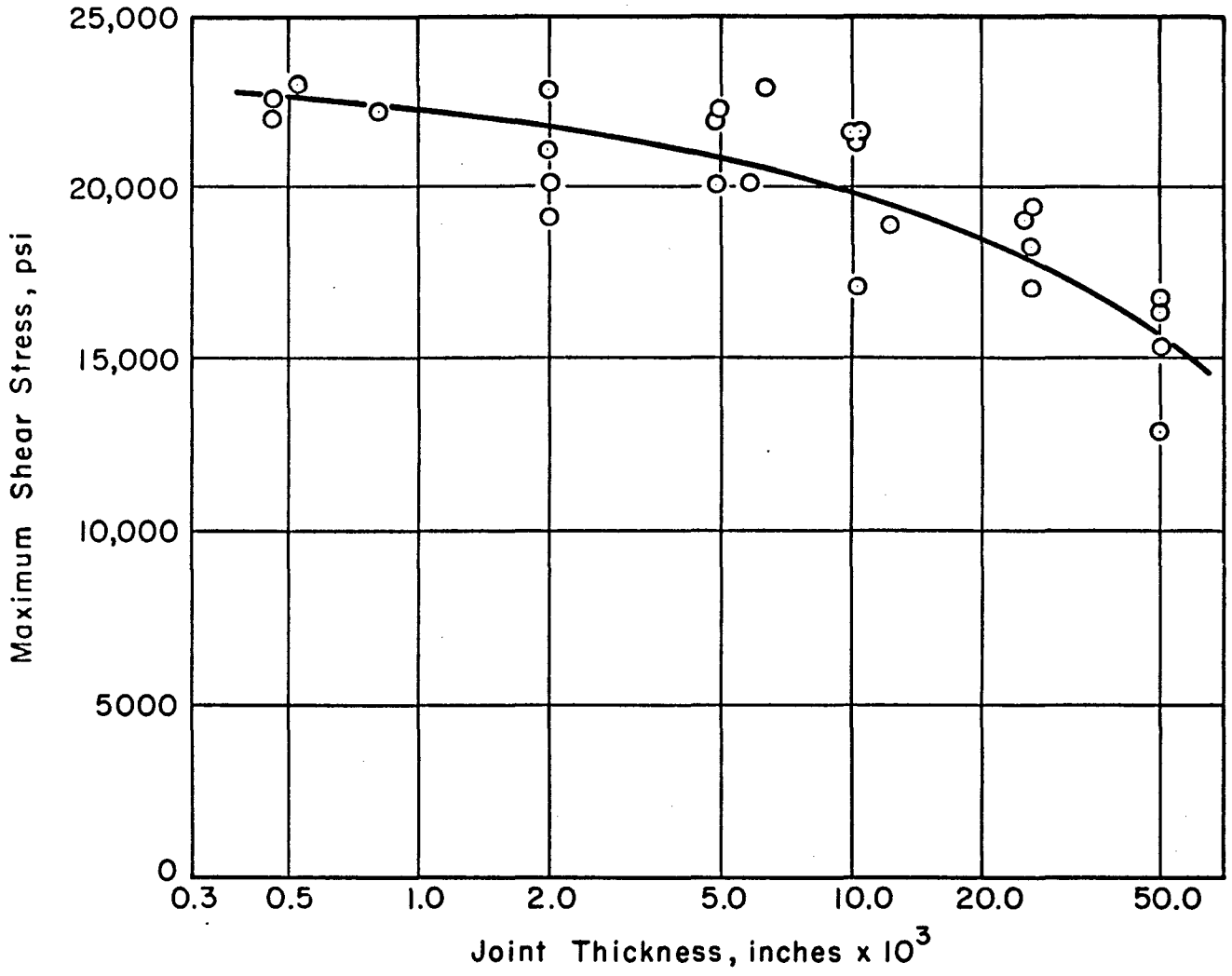

Fig. 7 Maximum Shear Stress for Silver Joints as a Function of Joint Thickness

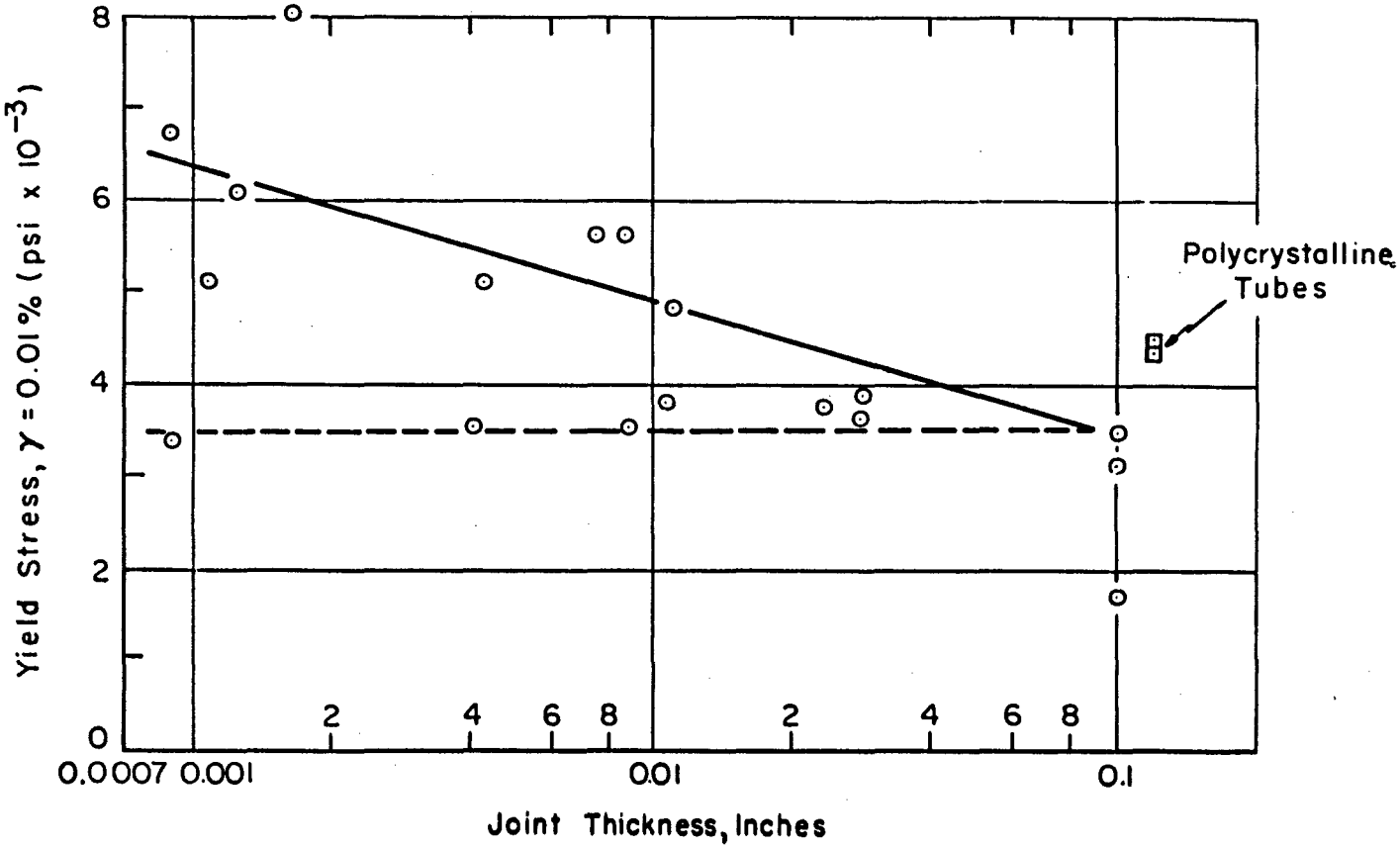

Fig. 8 Variation of Yield Stress, $\gamma = 0.01\%$, with Silver Joint Thickness

10^{-6} to 4×10^{-4}, Fig. 9. The large differences in yield strength are then associated with relatively small differences in slope of the τ vs $\gamma^{\frac{1}{2}}$ curve, in the microstrain region.

Although parabolic hardening behavior has been observed in polycrystalline metals, the effect is ascribed to the difference in yield characteristics of the several grains as dictated by their orientation relative to the tensile axis.[18] The few grains present in the brazed silver joints preclude consideration of this explanation. If it is assumed that slip in the joint is initiated near the steel interface to accommodate the discontinuity in elastic strain due to the higher modulus of the steel, a reasonable argument can be made for the observed behavior. For parabolic hardening can then be rationalized from the properties of piled up groups of dislocations. In this approximate treatment, the effect of the higher modulus steel on the dislocation pileup[16] will be neglected, and the relations determined by Eshelby, Frank and Nabarro[10] for dislocations piled up against a blocked dislocation in a homogeneous medium are assumed to apply.

The shear strain γ in a thin silver joint is:

$$\gamma = \frac{2\pi r \delta}{t} \tag{2}$$

where r = joint radius

t = joint thickness

δ = relative displacement per unit length along the circumference, of the two steel interfaces

The displacement per unit length, δ, is given by the number of active slip planes for unit length times the average shear produced by each. If δ is assumed for simplicity to result from shear of a series of slip planes making a constant angle θ with the interface

$$\delta = SN \cos\theta \tag{3}$$

where S = shear displacement per slip plane

N = number of active slip planes per unit length.

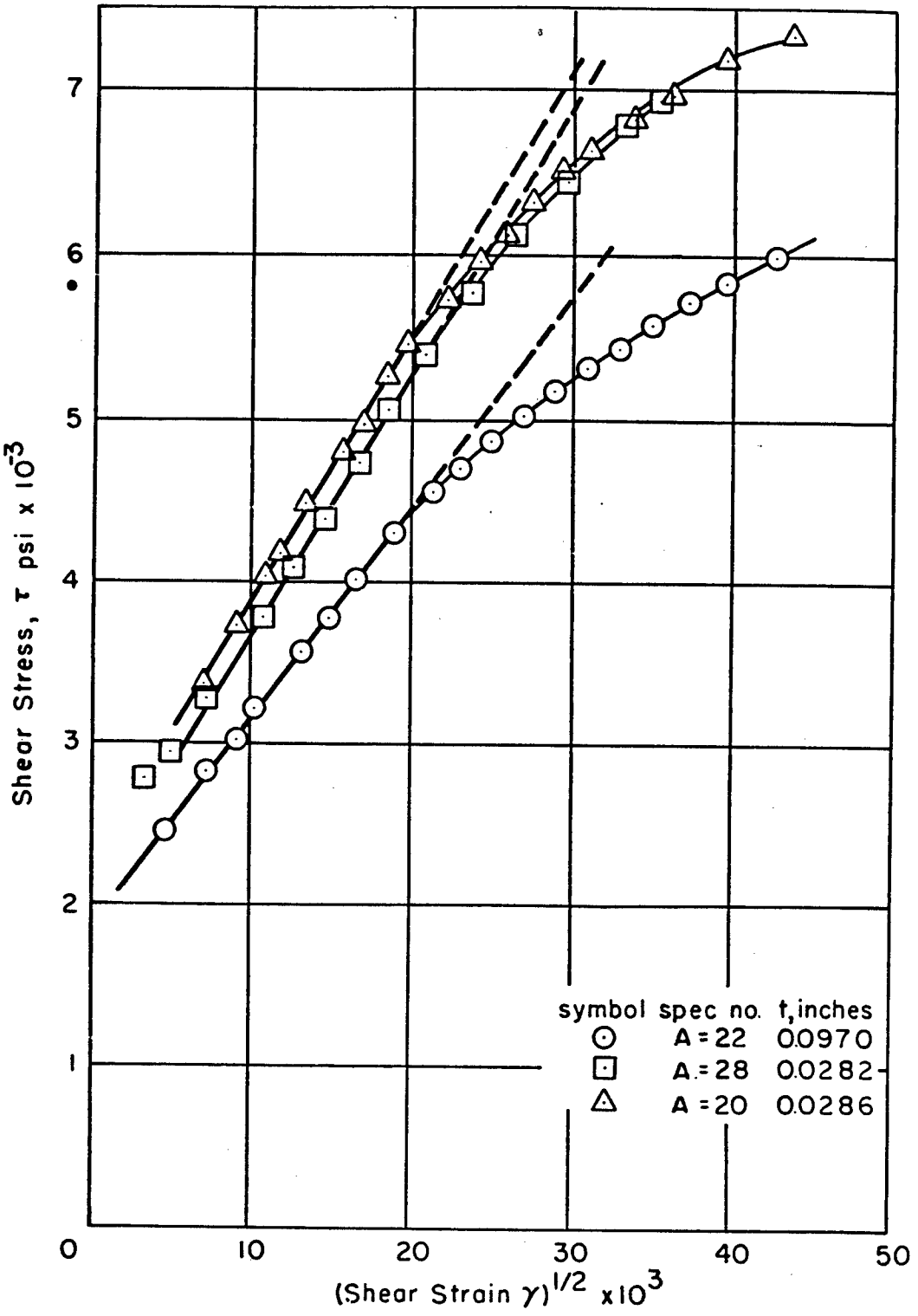

Fig 9 Parabolic Hardening During Initial Plastic Straining of Silver Joints ($10^{-6} < \gamma < 4 \times 10^{-4}$)

The displacement resulting from a group of N piled up dislocations on a slip plane under a stress τ_r is equivalent to the displacement due to a single dislocation of strength nb located 3/4 of the way from the source to the tip of the pileup (neglecting the steel interaction). Therefore:

$$S = 3/4\ Lnb \tag{4}$$

and

$$n = \frac{\pi(1-\nu)L\tau_r}{\mu b} \tag{1}$$

where the resolved shear stress $\tau_r = \tau_a \cos\theta$.

At small strains, it is observed that the slip line spacing in pure metals is uniform and a linear function of the reciprocal of the stress.[19,20] The measured spacing is closely approximated by the calculated minimum spacing that dislocations can pass one another under a given stress. Using this relationship for edge dislocations:[21]

$$N = \frac{8\pi(1-\nu)\tau_r}{\mu b} \tag{5}$$

Determining δ from Equations 4, 1 and 5, and inserting it in Eq. 2 gives

$$\gamma = K\tau^2$$

$$K = \left(\frac{2\pi r}{t}\right)\left(\frac{6L^2\pi^2(1-\nu)^2\cos^3\theta}{\mu^2 b}\right) \tag{6}$$

Applying Eq. 6 to the data for Fig. 9 should allow a rough approximation of the length L and number n of dislocations in the interface pileup before general yielding occurs in the joint. For specimen A-20, Fig. 9, the slope of the parabolic hardening line gives $\sqrt{K} = 6.2 \times 10^{-6}\ \text{psi}^{-1}$. Arbitrarily assuming $\theta = 45^\circ$, the

calculated length of the pileup of dislocations against the steel interface, $L = 10^{-4}$ inches and n of the order of 10 dislocations at the yield stress.

Inclusion of the elastic repulsion of the steel interface on the dislocation pileups in the silver will alter these conclusions in two ways. The equilibrium length of a pileup of n dislocations under a stress τ_r, Eq. 1, will be decreased. And the center of gravity of the pileup, Eq. 4, will be shifted away from the interface resulting in a smaller shear per slip line. However, Head's Analysis[16] noted in the introduction demonstrates that both these effects will be of relatively small magnitude, and the assumed approximation is not badly in error for a joint between steel and silver with $\mu_2/\mu_1 \cong 3$.

Applying this result in explanation of the yield stress data of Fig. 8, it will be noted first that the rate of initial hardening at small strains, and thus the yield stress, is dependent upon grain orientation. Changing the angle θ between the active slip plane and the steel interface will alter the parabolic hardening constant K through the relationship given in Eq. 6. And second, when the joint thickness is decreased to the order of the equilibrium pileup distance L, the yield stress should increase, since a decrease in L will reduce the number of piled up dislocations at a given stress (Eq. 1) and, therefore, decrease the shear strain. The limiting joint thickness in these experiments is possibly slightly large to show this effect.

In this regard, it is interesting to note that sintered fine powder silver-tungsten composites prepared in this laboratory also showed initial parabolic hardening in a tensile test, Fig. 10. For constant silver volume fraction, the mean spacing in the silver increases with increasing tungsten particle size from 4×10^{-5} to 2×10^{-4} inches. If these data are converted to τ and γ, assuming the average slip plane lies at 45° to the tensile

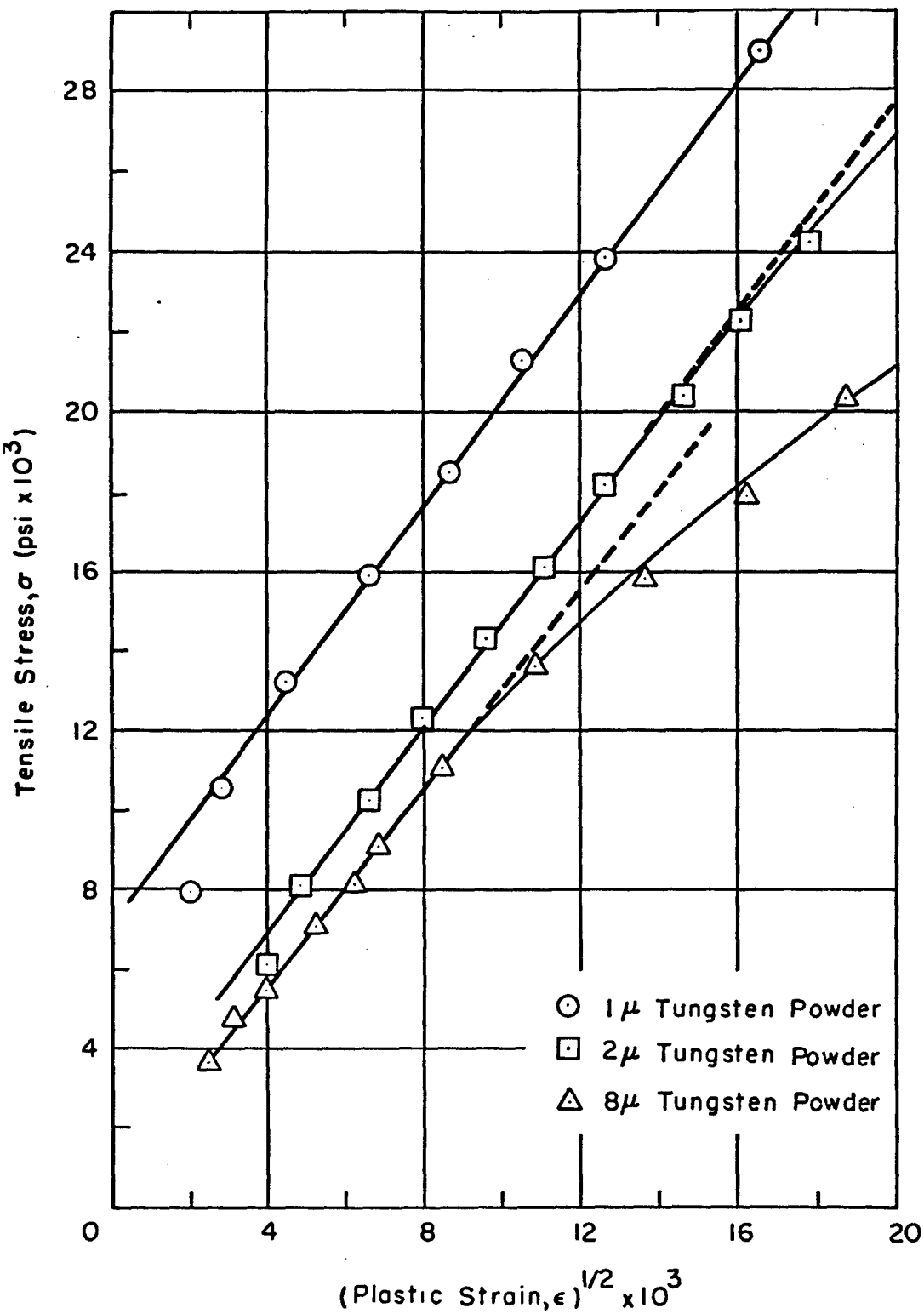

Fig 10 Parabolic Hardening During Initial Plastic Straining of Tungsten Powder Composites Containing 50 Vol % Silver

axis, the slope of the $\sqrt{\gamma}/\tau$ line is found to be of the same order of magnitude as that of the shear tests in Fig. 9, and the yield stress, at $\gamma = 10^{-4}$, rather higher. It is very probable that the postulated mechanism of stress promotion at small strains is general to the matrix behavior in composite materials.

C. Plastic Deformation in Silver Joints

Microscopic observations of individual grains of the silver joints during deformation showed a diversity in plastic behavior dependent upon the grain orientation relative to the steel interfaces. Although grain orientations were not determined, this factor appears responsible for the spread in τ-γ curves for specimens of the same joint thickness.

The extremes in observed deformation are well illustrated in Fig. 11 in two grains at a strain γ=1. The steel interfaces appear at the top and bottom of each figure and the scribed line across the figure was originally straight and parallel to the axis of twisting. The shadow just inside the interface results from a slight undercutting of the silver during polishing. In Fig. 11A, the strain is almost homogeneous. One slip system in this grain is parallel to the steel interface, as demonstrated by the prominent slip lines, and the deformation bands lying parallel to the scribe line. Fig. 11B shows the degree of strain inhomogeneity which can be developed in the presence of the steel interfaces. The initial orientation of this grain, from slip line traces, showed the (001) lying 19° below and 12° to the right of a standard projection in the plane of the photograph, with steel at the north and south poles. All slip planes intersect the interfaces. At the average strain γ=1 and stress τ = 14800 psi, the strain at the joint midplane is measured as γ = 3.40. At a distance 0.0015 inches from the upper interface, however, the strain is only γ = 0.10. Thus, the τ-γ behavior of the silver near the upper

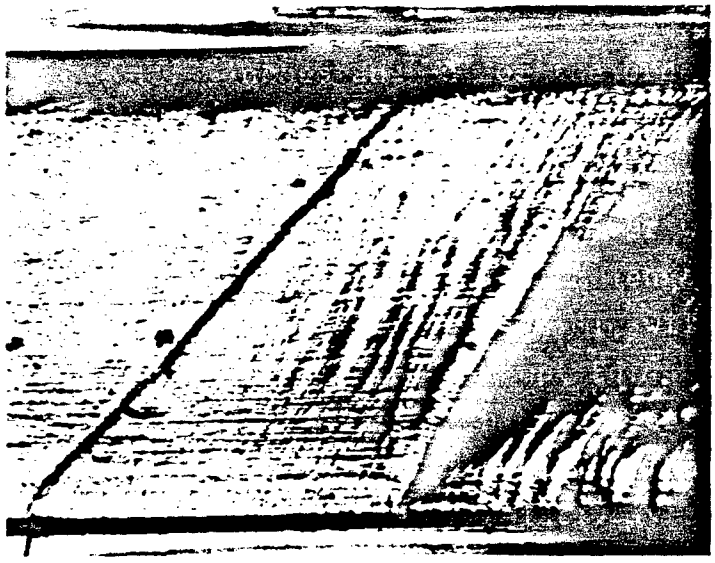

A. 0.025 inch joint x 75, homogeneous strain

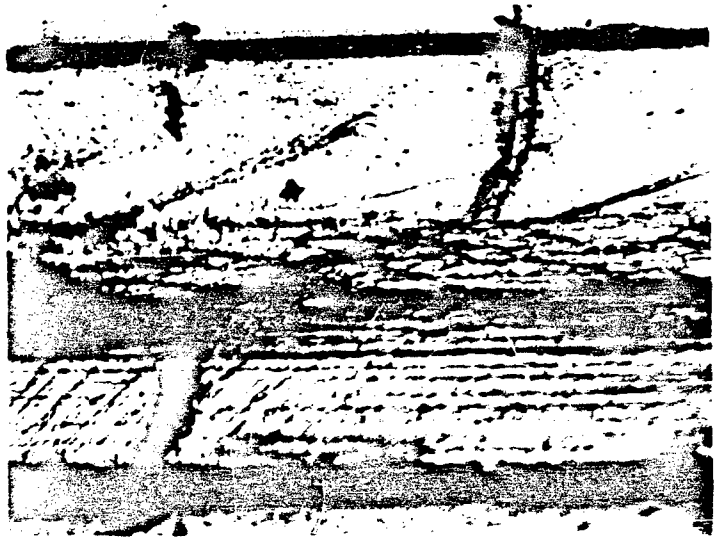

B. 0.010 inch joint x 200, inhomogeneous strain

Fig 11 Shear Deformation across Joint Grains at 100% Strains

interface is the same as the stronger of the 0.001 inch joints shown in Table I, though the width of this joint is 0.10 inches.

The majority of the grains in the deformed silver joints showed this behavior to a greater or lesser extent. In general, strain was restricted over one half to two thirds of the joint width and highly concentrated in the central region. This accounts for the higher work hardening rate of the brazed silver joints as compared with the fine grained polycrystalline silver.

Further examples of inhomogeneous deformation in thinner joints are shown in the fractured grains of Fig. 12.* Even at stresses in excess of 20,000 psi, the strain in the interface region remained very limited.

The inhomogeneous straining of a brazed joint in shear was first observed by Bredzs and Schwartzbart.[22] These workers attributed the limitation of strain near the steel interface to the same factors responsible for the strength of the brazed joint in tension. However, the present series of results shows that strengthening in the two cases arises from distinctly different sources. A joint in tension is highly resistant to deformation because the ductile wafer is constrained from contracting along its diameter normal to the tensile axis since it is bonded to the stronger non-deforming metal. Thus, a high hydrostatic stress component is induced in the ductile wafer.[17] The shear joint strains inhomogeneously, on the contrary, because the requirement of strain continuity at the non-deforming interface affects the work hardening characteristics of the ductile joint metal at a considerable distance from the interface. Since slip in the ductile joint is blocked at the interface, deformation in this region must occur by the operation of greater numbers of slip

*The line in Fig. 12B was scribed at an angle to the twist axis.

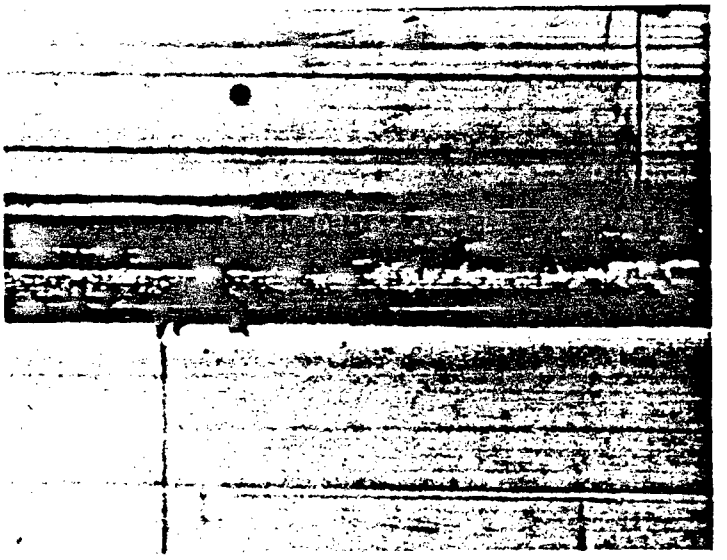

A. 0.002 inch joint x 300

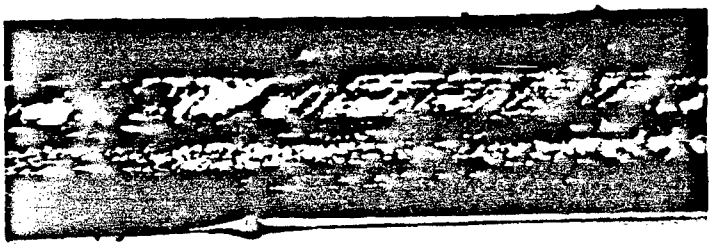

B. 0.005 inch joint x 200

Fig. 12 Ductile Fractures at Midplane of Joints

systems over shorter slip distances. This leads to a higher rate of work hardening in a manner analogous to the hardening of polycrystalline metals discussed in the introduction.

The work hardening rate of the silver joints exceeds that of polycrystalline silver because local stresses due to dislocation pileups cannot be relaxed across the non-deforming interface. Thus, the dislocation content in the interface region rises rapidly at small strains, resulting in rapid hardening.

An example of slip line development during joint deformation is shown in Fig. 13. At small strains (13A) the slip lines are observed to be long and continuous, penetrating close to the steel interface. As the strain is increased (13B) further long slip bands form in the central region of the joint, while the slip band concentration near the interface remains almost unchanged. At large strains (13C) slip is heavily concentrated in the central joint area. In the well lighted regions near the interface it is apparent that the number of visible slip bands has not appreciably increased. The additional slip that has accrued there must arise from fine scale multiple slip which results in rapid work hardening.

It will be seen from these results that the strength of a joint grain in shear is dependent both on its orientation relative to the steel interfaces, and on its thickness. If one slip system of the grain is almost parallel to the interface, shear strain may be almost homogeneous across the joint, and shear resistance low. If all slip systems intersect the interface at a reasonable angle, strain may be limited over a large fraction of the joint volume adjacent to the interface, forcing large strain accommodation in a narrow midplane region at higher stresses. The physical limitations in making accurately spaced thin brazed joints precluded production of joints much less than 0.001 inches. However, the trend of test results, the microscopic observations, and the basic strengthening process discussed above would indicate that thinner joints should show yet greater strength.

A. 4% strain

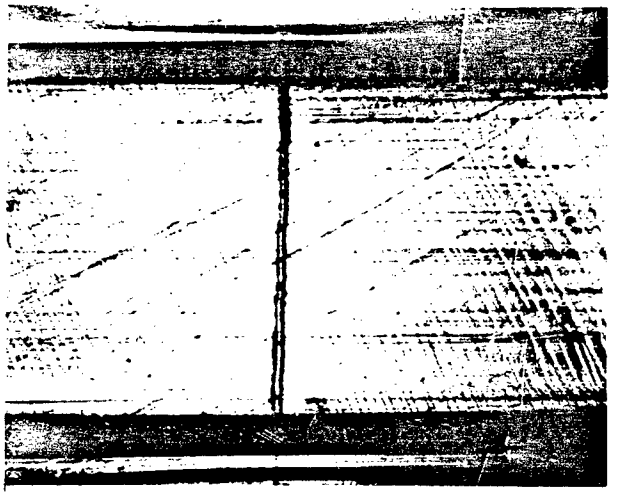

B. 10% strain

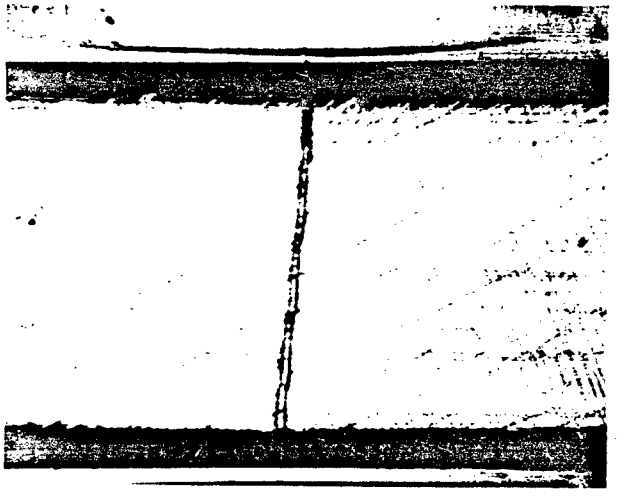

C. 100% strain

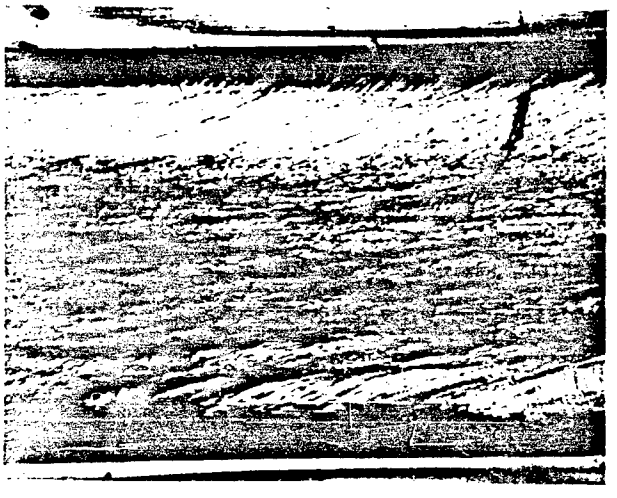

Fig 13 Slip Line Development During Inhomogeneous Grain Deformation x 75 0.025 Inch Joints

D. Plastic Deformation in Composite Materials

For composites of practical importance elements of the stronger phase are spaced in the softer matrix at mean distances of 5×10^{-4} to 4×10^{-5} inches,[1] 1/2 to 1/25 the 0.001 inch minimum joint thickness tested here. From the above results, the matrix phase will show an increased resistance to shear in the composite as well as a hydrostatic strengthening.

The work of Moffatt and Wulff[17] on thin brazed joints in tension demonstrated that the fracture strength of the matrix phase can be increased to as much as 4 times its normal ultimate tensile strength as the result of hydrostatic constraint. The shear joint data demonstrate a shear strength increase of 1 1/2 times the bulk polycrystalline strength. Moreover, microscopic observation of the shear behavior in the joint very close to the non-deforming interface indicates the probability that a shear resistance considerably greater than this is developed.

Thus, in contrast to elastic behavior, the strength developed on plastically deforming a composite material should be in excess of that predicted by a simple mixture rule based on the plastic behavior of the individual components.

CONCLUSIONS

A study of the yield and plastic behavior of thin ductile silver joints bonded to rigid steel interfaces, and a comparison of this behavior with the deformation of a free grained polycrystalline aggregate revealed the following distinctions:

1. Early plastic straining of a thin joint ($\gamma < 4 \times 10^{-4}$) follows a parabolic hardening law. This behavior can be explained by a proposed model for strain initiation invoking dislocation pileups against the interface.

2. During subsequent plastic deformation, the strain across the thin joint grains is, in most cases, extremely inhomogeneous. A region of limited strain extends from each interface over 1/4 to 1/3 of the joint width. The average strain of the grain is accommodated by exaggerated shearing in the central 1/2 to 1/3 of the joint.

3. The effect of inhomogeneous plastic straining is to increase the work hardening rate of the ductile joint to 1 1/2 to 2 times that of fine grained polycrystalline silver. This increase in hardening rate was observed equally for joints in which the minimum grain dimension was over ten times the polycrystalline grain size, as in the thinner joints.

4. The inhomogeneous straining, and resulting higher strength of the silver joints, are postulated to arise from two factors:

a. The requirement of strain continuity at the interface between steel and silver induces a region of short range multiple slip near the interface which increases the work hardening.

b. Because localized shear stresses are not relaxed across the rigid interface, the dislocation density in the interface region increases rapidly with strain.

REFERENCES

1. Gurland, J., and Bardzil, P., "Relation of Strength, Composition and Grain Size of Sintered WC-Co Alloys," Trans. AIME V 203 (1955), p. 311

2. Nishimatsu, C., and Gurland, J., "Experimental Survey of the Deformation of the Hard-Ductile Two-Phase Alloy System WC-Co," Trans. ASM V 52 (1960), p. 469

3. Taylor, G. I., "Analysis of Plastic Strain in a Cubic Crystal," Stephen Timoshenko 60th Anniversary Volume, Macmillan Co. (1938), p. 218

4. Bishop, J.F.W., and Hill, R., "A Theory of the Plastic Distortion of a Polycrystalline Aggregate under Combined Stresses," Phil. Mag. V 42 (1951), p. 414; "A Theoretical Derivation of the Plastic Properties of a Polycrystalline Face-Centered Cubic Metal," Phil. Mag. V 42 (1951), p. 1298

5. Kocks, U. F., "Polyslip in Polycrystals," Acta Met. V 6 (1958), p. 85

6. Boas, W., and Hargreaves, M. E., "On the Inhomogeneity of Plastic Deformation in Crystals of an Aggregate," PRS VA 193 (1948), p. 89

7. Urie, V. M., and Wain, H. L., "Plastic Deformation of Coarse Grained Aluminum," J. Inst. Met. V 81 (1952-53), p. 153

8. Boas, W., and Ogilvie, G. J., "The Plastic Deformation of a Crystal in a Polycrystalline Aggregate," Acta Met. V 2 (1954), p. 655

9. Jaswon, M. A., and Foreman, A.J.E., "The Non-Hookian Interaction of a Dislocation with a Lattice Inhomogeneity," Phil. Mag. V 43 (1952), p. 201

10. Eshelby, J. D., Frank, F. C., and Nabarro, F.R.N., "The Equilibrium of Linear Arrays of Dislocations," Phil. Mag. V 42 (1951), p. 351

11. Livingston, J. D., and Chalmers, B., "Multiple Slip in Bicrystal Deformation," Acta Met. V 5 (1957), p. 322

12. Hauser, J. J., and Chalmers, B., "Plastic Deformation of Bicrystals of F.C.C. Metals," Acta Met. V 9 (1961), p. 802

13. Armstrong, R., Codd, I., Douthwaite, R. M., and Petch, N. J., "The Plastic Deformation of Polycrystalline Aggregates," Phil. Mag. V 7 (1962), p. 45

14. Honeycombe, R.W.K., and Boas, W., "The Deformation and Recrystallization of an Alloy Containing Two Phases," Australian Journal of Scientific Research, V A1 (1948), p. 70

15. Clarebrough, L. M., "Deformation and Recrystallization of Alloys Containing Two Phases," Australian Journal of Scientific Research, V A3 (1950), p. 73

16. Head, A. K., "The Interaction of Dislocations with Boundaries and Surfaces," Australian Journal of Physics, V 13 (1960), p. 278

17. Moffatt, W. G., and Wulff, J., Tensile Deformation and Fracture of Brazed Joints, Office of Scientific Research Report AFOSR 2292, ASRL TR 94-1, Sept. 1961, to be published, Welding Journal Research Supplement.

"Strength of Silver Brazed Joints in Mild Steel," Trans. AIME V 209 (1957), p. 442

18. Brown, N., and Lukens, K. F., Jr., "Microstrain in Polycrystalline Metals," Acta Met. V 9 (1961), p. 106

19. Brown, A. F., "Surface Effects in Plastic Deformation of Metals," Advances in Physics V 1 (1952), p. 427

20. Wilsdorf, D. Kuhlman, and Wilsdorf, H., "The Surface Structures of Deformed Aluminum, Copper, Silver and Alpha-Brass and their Theoretical Interpretation, Acta Met. VI (1953), p. 394

21. Cottrell, A. H., Dislocations and Plastic Flow in Crystals, Oxford University Press (1953), p. 152

22. Bredzs, N., and Schwartzbart, "Fundamentals of Brazing," Sixth Final Report, Armour Research Foundation, Contract No. DA 11-022,ORD-957, Ordnance Project No. TB4-31 (ARF Project No. B-039), Frankford Arsenal

APPENDIX

A highly sensitive torsion testing apparatus was developed to study the shear behavior of thin silver joints brazed in tubular steel specimens. The apparatus allowed accurate measurements of plastic strains of 2×10^{-4} in the silver for joints 0.001 inches thick, and strains as great as 1 in joints one hundred times this thickness. Misalignment constraints and the attendant bending effects and hydrostatic constraints were virtually eliminated by specially designed specimen grips. The accuracy and versatility of this unit suggest application to a wide range of torsion testing problems.

The testing unit was a manually operated gear driven lathe modified with additional gears on the headstock to allow a complete rotation of the calibrated hand wheel for 1 degree twist on the specimen. Torque was transmitted between a Jacobs Chuck in the headstock and two orthogonal sets of ball bearings in the tail-stock which allowed continuous specimen self-alignment.

The specimen with the thin brazed joint in the central quarter inch reduced section is shown in Fig. 1b. Extension pieces, Figs. 1a and 1c, were screwed into the ends of the specimen, contacting uniformly over the squared surfaces, and tightened individually with a strap wrench. The headstock extension, Fig. 1A, was a thin-walled stainless steel tube which served also for torque measurement with two 90^{o} rosette type etched foil strain gages mounted centrally 180 degrees apart. The combined gage output, measured on a Baldwin SR-4 strain indicator, was directly proportional to the applied torque. Dead loading calibration showed a shear stress sensitivity of $\pm$ 10 psi on a typical specimen.

The second specimen extension engaged a dog in the tail-stock by means of the self-aligning coupling designed to transmit torque but not bending moment. Fig. 2A shows a general view of

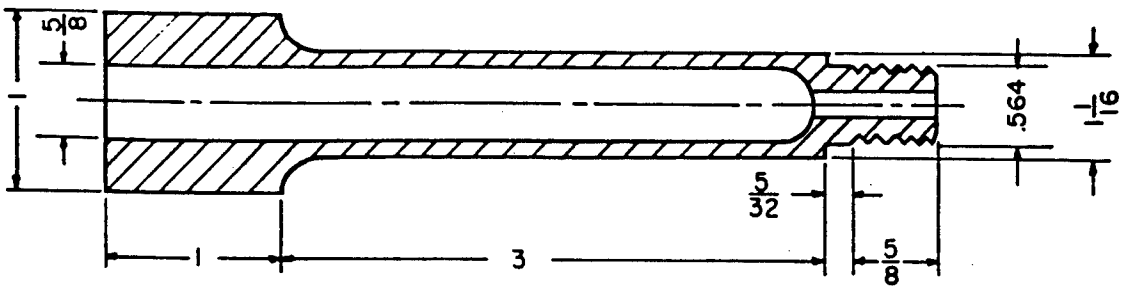

FIG 1A

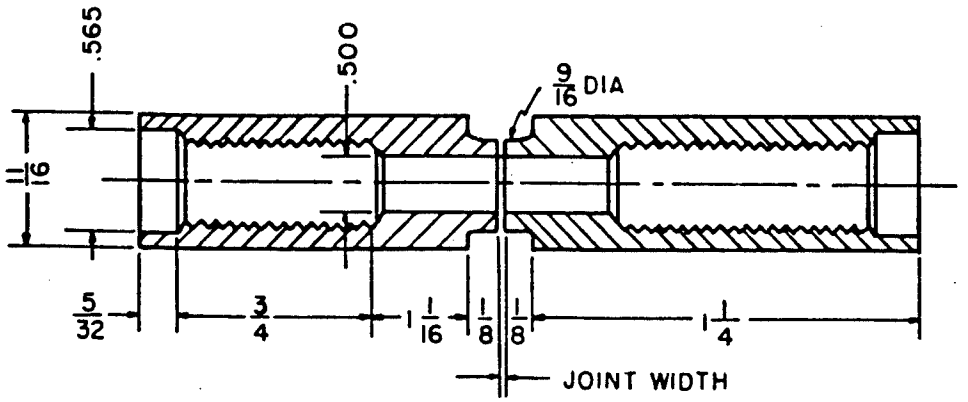

FIG 1B

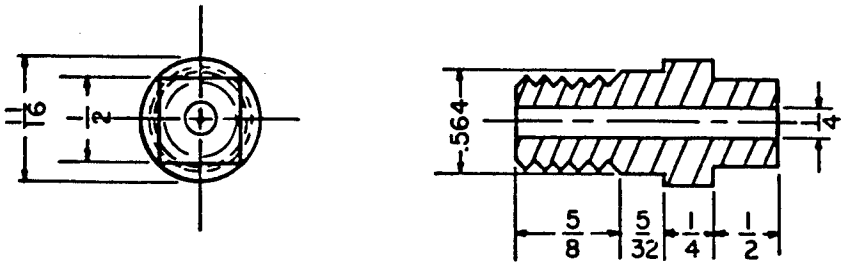

FIG 1C

FIGURE 1A TORSION SPECIMEN AND THREADED END EXTENSIONS

A) HEAD STOCK EXTENSION AND TORQUE MEASURING TUBE

B) TORSION SPECIMEN

C) TAIL STOCK EXTENSION

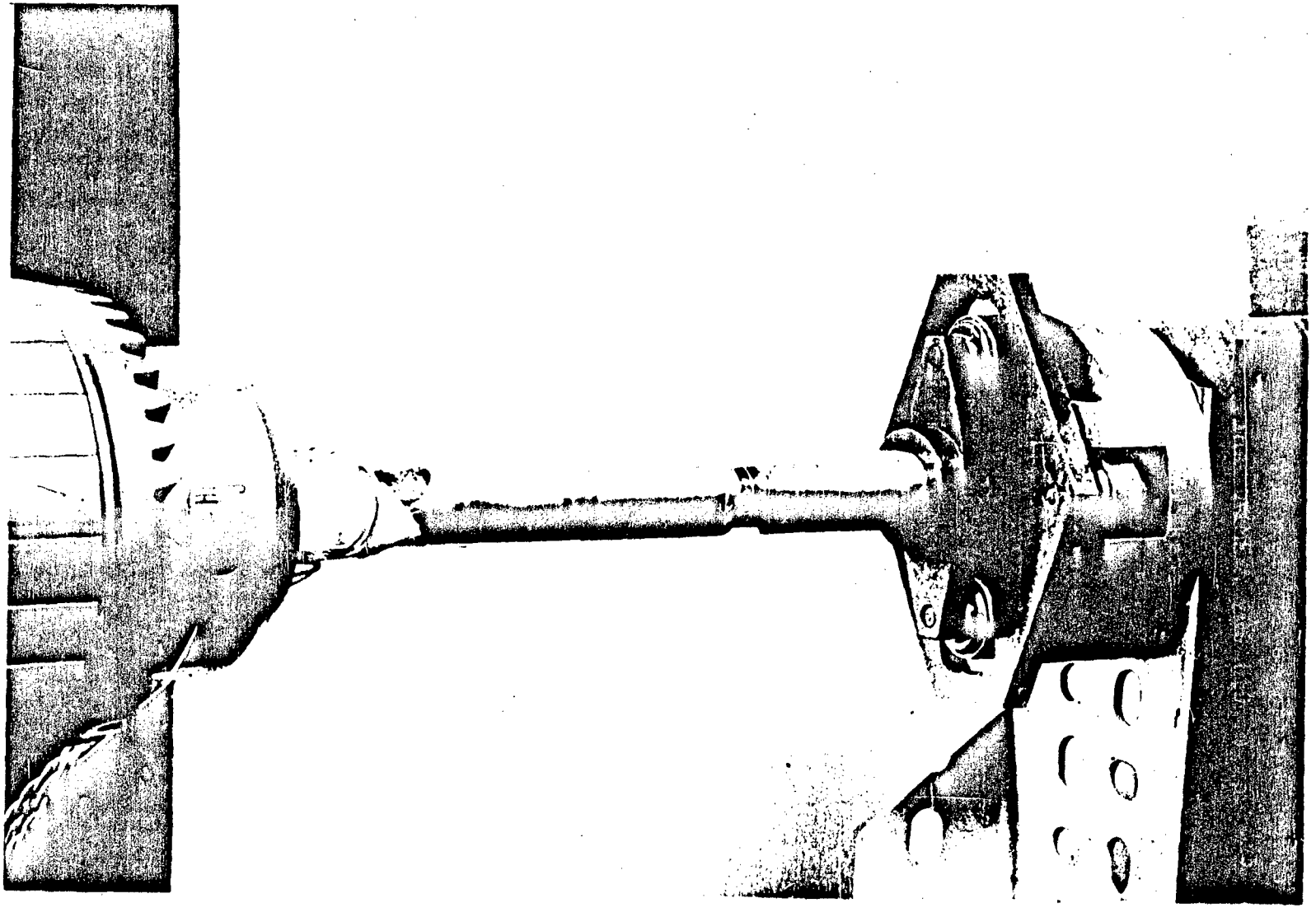

Fig. 2A View of a specimen mounted between its extension pieces, and of the tailstock coupling designed to transmit torque but no bending stresses

this coupling, consisting of orthogonally aligned sets of ball bearings. Also shown are the torque tube mounted in the headstock, and a specimen. The tail-stock extension, greased with molybdenum disulfide slid directly into a square hole in the torque transmitting coupling. The specimen and its extension pieces thus formed a cantilever supported by the lathe headstock. The only bending stress on the joint resulted from the weight of half the specimen, the lighter portion of the extensometer and the outer extension piece. This weight caused a small elastic strain in the joint which, by the principal of elastic superposition, did not influence the strains obtained by the application of torque except very close to the yield point where their presence slightly modified the yield locus for different parts of the joint. The coupling also allowed free axial motion of the specimen during torsion.

The necessary sensitivity of the electro-mechanical extensometer was predetermined by the accuracy required to measure strain in the thinnest joint. The designed apparatus had a linear electric output of two volts per degree of twist, readable with attendant instrumentation to $\pm$ 1 mv. This corresponds to a strain of $\pm$ 0.02 percent in a 0.001 inch joint, and $\pm$ 0.002 percent in a joint 0.100 inches wide.

The desired strain sensitivity was obtained by applying the twist across the joint to the rotor of a Transipot Variable Reluctance Rotary Motion Potentiometer* with the stator of the potentiometer held fixed at the joint edge. The complete extensometer is shown in Fig. 3A. The potentiometer at the upper left of the figure was supported on the shoulder of the specimen by two precision ball bearings in a frame. The freely rotating support allows positioning of the potentiometer by two double pointed knife edges indented into the reduced section of the steel about

* Transipot Model 15R30-1, Arnoux Corp., Los Angeles, California

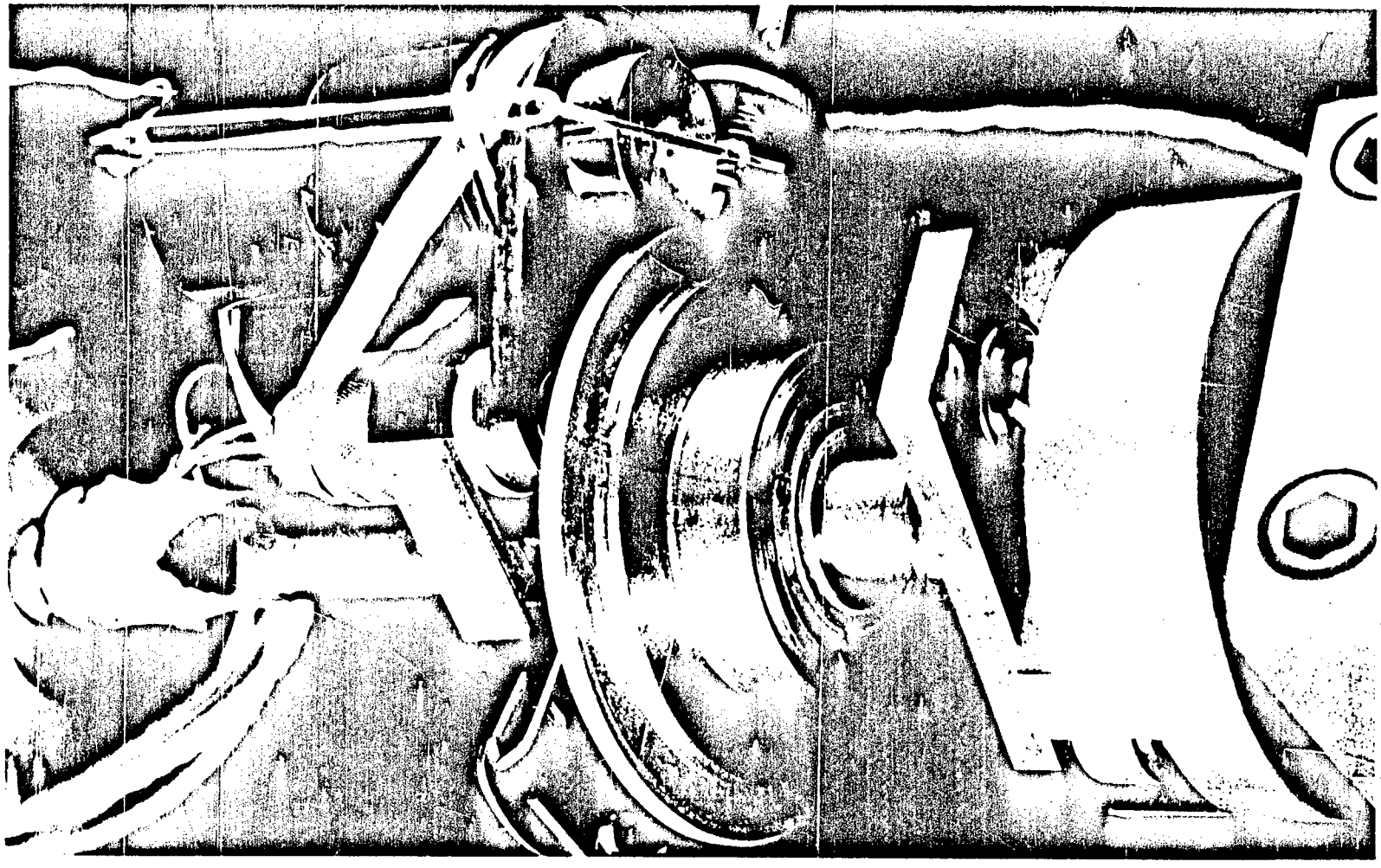

Fig. 3A View of the twist measuring apparatus set up as for a test

0.01 inches from one edge of the joint. The positioning knife edges and potentiometer support are shown mounted on a sectioned specimen in Fig. 4A.

Motion across the joint was applied to the 3/4 inch diameter polished stainless steel disc fixed on the potentiometer rotor by a 3-inch polished hard rubber wheel (Fig. 3A). The wheel, supported on the opposite specimen shoulder on double ball bearings, was positioned by a single pin with a beveled point indented 0.01 inches from the other edge of the joint. By arranging the support of the extensometer independent of the positioning pins, it was possible to minimize the volume of elastically stressed steel included in the measurement of the strain of the silver joint.

The extensometer was calibrated over its 30 degree usable range by measuring the voltage change for a series of large, accurately determined angular displacements (one-half to one degree). The accuracy and linearity of the calibration were then checked by repeated determinations of the shear modulus of tubular steel samples tested to the yield point. Modulus measurement also served to demonstrate that no bending strains were imposed upon the specimen during twisting since bending induced an artificial increase in the measured elastic strain for the chosen extensometer geometry.

Average measured shear modulus for five 1020 steel specimens was 11.4×10^6 psi with a sampling variation of $\pm$ 2 percent. Repeated measurements on a single sample demonstrated that the largest error arose from determination of the exact distance between measuring points. This error did not, of course, affect plastic strain measurements on the silver joint specimens. For a series of over 50 measured points in any steel modulus determination, strain readings deviated by less than $\pm$ 1 unit in the least reading from the average curve, and overall linearity was within $\pm$ 2 percent for stresses greater than 150 psi.

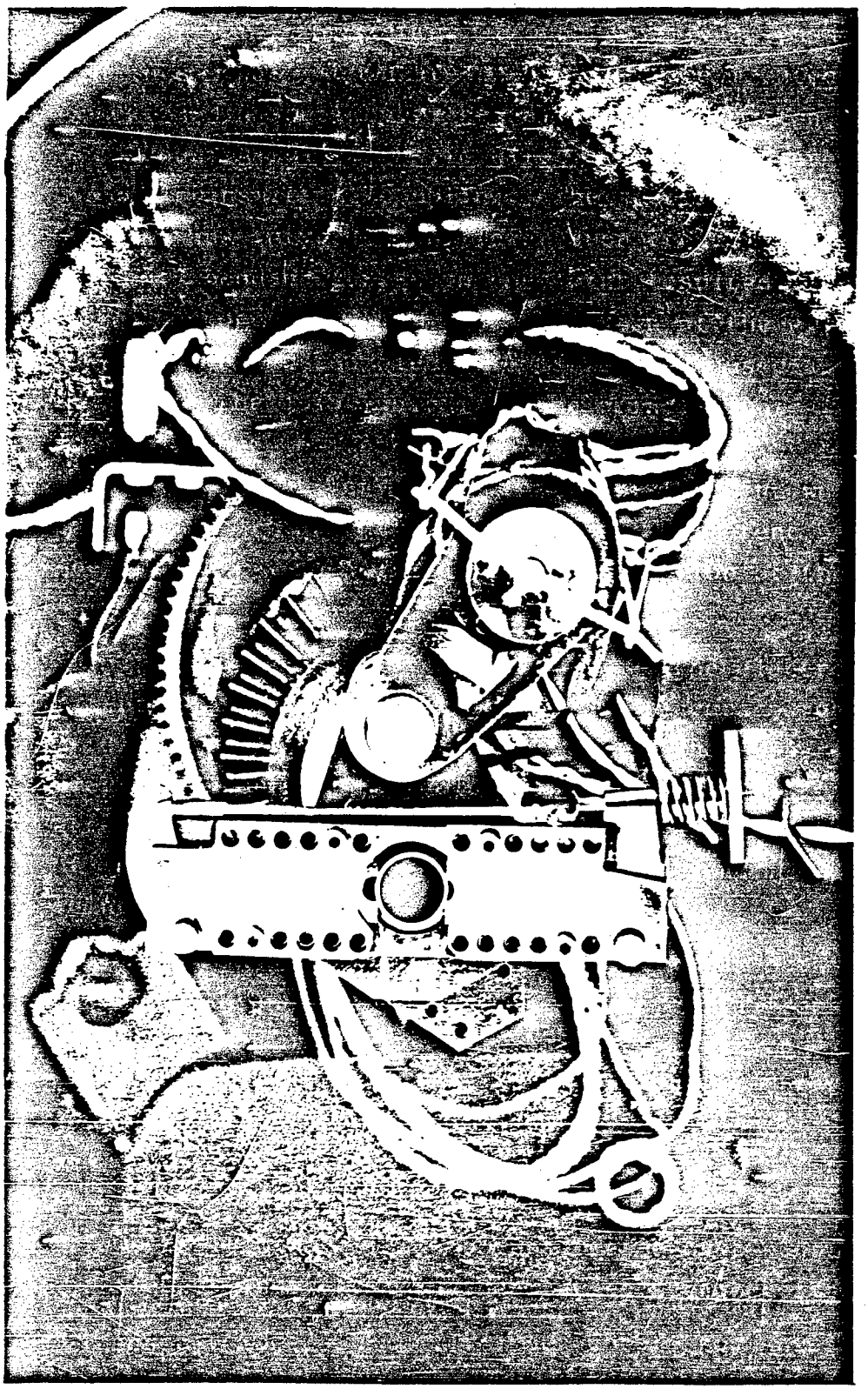

Fig. 4A The headstock end part of the twist measuring apparatus mounted on the headstock end of a fractured specimen

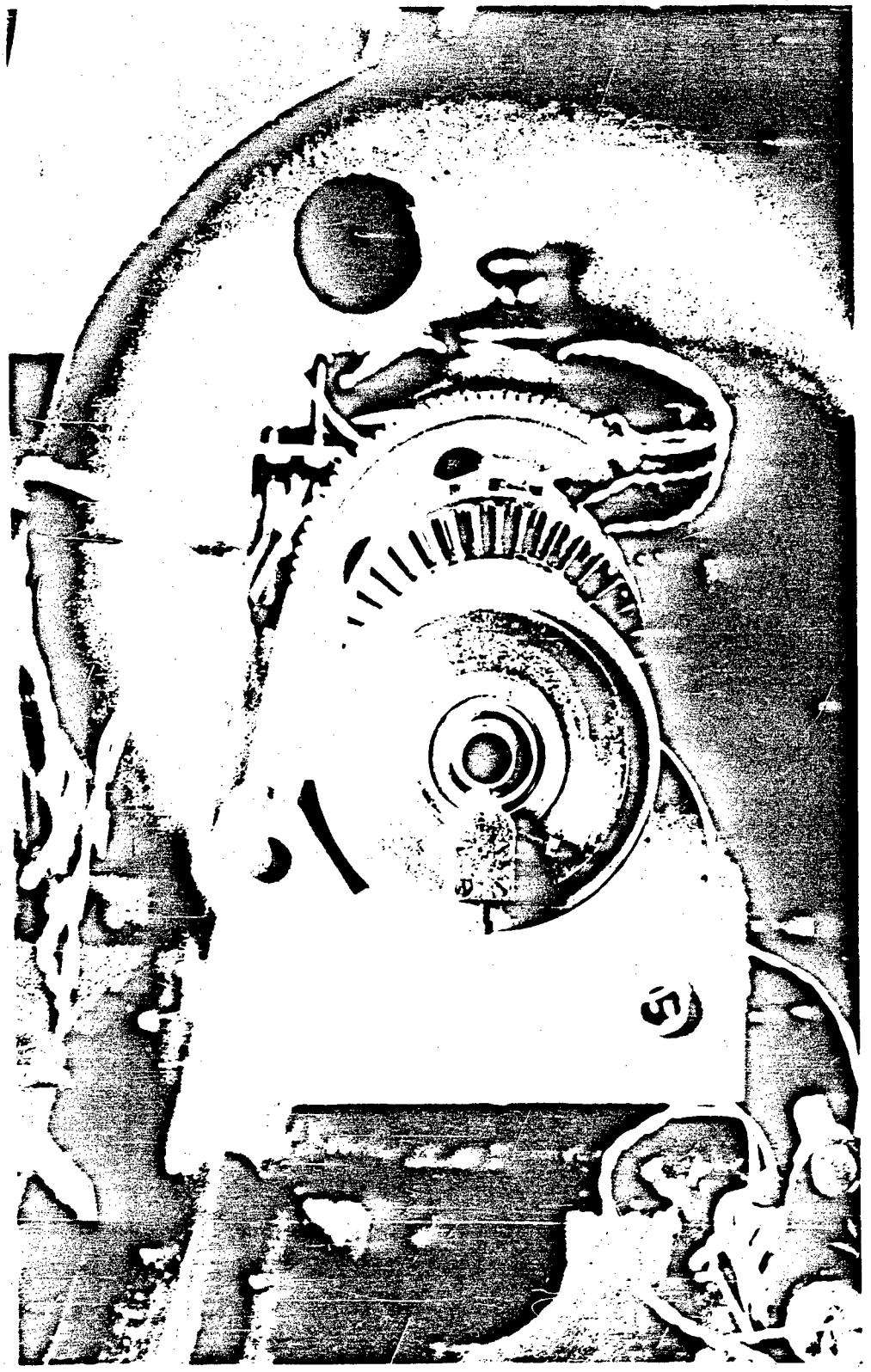

Fig. 5A The tailstock end part of the twist measuring apparatus, mounted on the headstock end of a fractured specimen for photographing

During initial elastic straining of both the steel and silver joint specimens, strain deviations to either the right or left of the true modulus line were observed in individual cases. The anomalous behavior apparently resulted from the seating of the extensometer positioning pins. In all cases, correct modulus determinations could be made after the shear stress exceeded 1500 to 2000 psi.

A block diagram of the electrical circuitry for the extensometer is shown in Fig. 6A. The Transipot transducer was fed with stabilized 400 cycle current at 26 volts through an impedance matching network. The demodulated DC output of the Transipot was measured on a potentiometer sensitive to 0.1 mv. A range multiplication switch allowed measurement of large strains at appropriately lower sensitivity.

Extensive experience with the torsion testing apparatus described has shown the unit not only capable of a high degree of sensitivity but soundly reliable if proper care is taken in its setup and use. Principal difficulties were associated with strain inaccuracies resulting either from loose fitting extensometer positioning pins or from fracturing of the positioning pin points. These difficulties were overcome by hand-lapping the pins to an exact fit in their holders, and, before each test, grinding and polishing the joints into exact alignment.

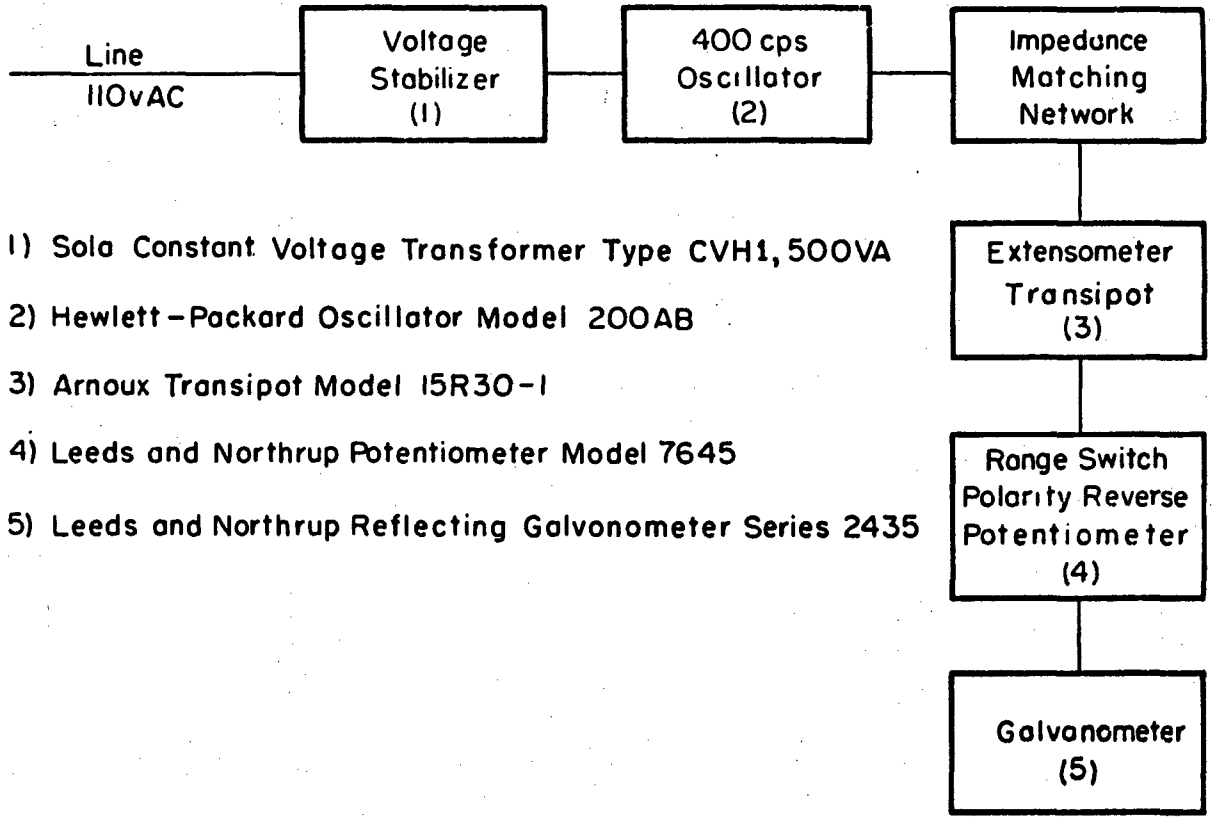

1) Sola Constant Voltage Transformer Type CVH1, 500VA

2) Hewlett-Packard Oscillator Model 200AB

3) Arnoux Transipot Model 15R30-1

4) Leeds and Northrup Potentiometer Model 7645

5) Leeds and Northrup Reflecting Galvonometer Series 2435

Fig 6A Block Diagram of Extensometer Circuitry